

Weather Related Continuity and Completeness on Deep Space Ka-band Links: Statistics and Forecasting

Shervin Shambayati
Jet Propulsion Laboratory, California Institute of Technology
4800 Oak Grove Dr.
Pasadena, CA 91109
E-mail: *Shervin.Shambayati@jpl.nasa.gov*

Abstract— Due to lack of spectrum at 8.41 GHz (X-band) future NASA deep space missions will be using 32 GHz Ka-band. Since combating adverse weather events require prohibitively large margins at Ka-band, link design methods based on maximizing the average data return over the link subject to a minimum link availability have been proposed. Furthermore, weather forecasting has also been suggested as means of combating the weather effects on the link. While the performance of these methods in term of data return has been well-understood, questions have remained about the completeness and continuity performance of the link. In this paper the concept of link “stability” as means of measuring the continuity of the link is introduced and through it, along with the distributions of “good” periods and “bad” periods, the performance of the proposed Ka-band link design method using both forecasting and long-term statistics has been analyzed. The results indicate that the proposed link design method has relatively good continuity and completeness characteristics even when only long-term statistics are used and that the continuity performance further improves when forecasting is employed.

band operations as most X-band and S-band missions carried with them sufficient margin for other things as to negate or at least obscure the effects of the weather on the link. With Ka-band, however, it is expected that the dominant source of outages to be weather effects since the margin necessary to negate weather outages is so large as to be prohibitive. In the past we have proposed a methodology for optimally designing the Ka-band link according to the atmospheric noise temperature statistics subject to a minimum availability requirement [2], [3], [5]. In addition, we have shown how this technique could be used both with long-term statistics and forecasted distributions [4], [6]. In this paper we obtain the continuity and completeness performance of this methodology for both when forecasting is used and when long-term statistics are used and the results are compared with each other. The results indicate that the our proposed link design approach has good continuity characteristics even with long-term statistics. Furthermore, it is shown that while forecasting does not return much more data than the case where only monthly statistics are used, forecasting does improve the continuity of the link.

TABLE OF CONTENTS

- 1 INTRODUCTION
- 2 LINK DESIGN AND CONTINUITY EVALUATION
- 3 FORECASTING
- 4 RESULTS AND DISCUSSION
- 5 CAVEATS
- 6 CONCLUSIONS

1. INTRODUCTION

As NASA’s deep space missions begin to use Ka-band (32 GHz) frequency for their primary science data return, one of the more difficult issues to address has become that of data continuity and completeness for Ka-band. The problem with completeness and continuity at Ka-band is that they are dependent on link design philosophy, spacecraft capabilities and link geometry which could vary from mission to mission and even within a mission. In addition, NASA’s experience with X-band and S-band missions does not shed any light on Ka-

This paper is organized in the following fashion: Section 2 gives an overview of the link design methodology and introduces the concept of link “stability” as a way of measuring the link’s continuity performance. Section 3 explains how the forecasting algorithm provides atmospheric noise temperature probability distributions. In section 4, results of the analysis are discussed. In section 5 caveats are presented. In section 6 conclusions are summarized.

2. LINK DESIGN AND CONTINUITY EVALUATION

As mentioned in the previous section, continuity of a link is dependent on the link design philosophy that is employed as well as the elevation profile for the pass. In addition, spacecraft operational limitations (*e.g.*, number of data rates available, number of data rates that could be used during a pass, *etc.*) determine the link design as well. Therefore, an attempt to evaluate the continuity of the Ka-band link in general would be at best an approximation and the actual continuity of the link will vary on a case by case basis. In this paper, the approach that we take is to design the link for a four different elevations (10, 30, 60 and 80 degrees) using a link design approach that maximizes the average gain-to-temperature ratio (G/T) of the antenna subject to a minimum availability of

90%. This approach has been outlined previously, and a full discussion of it is presented in [2] and [3]. It suffices to say that with this design approach, for a given zenith atmospheric noise temperature (T_z) distribution, at a given elevation θ , the link design approach provides a design $T_z, T_z^{(0)}(\theta)$.

Given a times series of observations of T_z and a given link design temperature, $T_z^{(0)}(\theta)$, it is said that the link is in a “good” state (that is, the data could be received on the link with an acceptable error rate) if $T_z \leq T_z^{(0)}(\theta)$. Conversely, the link is said to be in a “bad” state (*i.e.*, the error rate on the link is unacceptable) if $T_z > T_z^{(0)}(\theta)$. The continuity of the link could be evaluated by gathering statistics on the duration of “good” and “bad” periods.

As much as gathering statistics on “good” and “bad” periods is helpful in understanding the continuity performance of the link, these statistics more often than not provide a skewed picture of the continuity on the link. This is because if for a period of time the link is marginal so that it switches between good and bad states many many times, then each of these short “good” and “bad” periods are counted in the statistics even though they cover a very short period of time. Therefore, it is better to look at the continuity of the link from a temporal point of view by answering the question “What fraction of the time is the link in a ‘good’ state such that the ‘good’ state duration is greater than or equal to τ hours?” The answer to this question not only identifies the fraction of the time that link is in a “good” state but also it points to the “stability” of the link when it is in the “good” state. To put this formally, let t_{obs} be the period over which the continuity of the link was observed. If there are N “good” periods during this time with $t_i^{(G)}$ indicating the duration of the i th “good” period, then we can define a “stability” function, $\Psi(\tau)$, as

$$\Psi(\tau) = \frac{\sum_{i=0}^N I_{\tau}(t_i^{(G)}) t_i^{(G)}}{t_{obs}} \quad (1)$$

where $I_{\tau}(x)$ is an indicator function of x given by:

$$I_{\tau}(x) = \begin{cases} 0 & x < \tau \\ 1 & x \geq \tau \end{cases} \quad (2)$$

The function in equation 1 allows us to see what fraction of a Ka-band track stays occurs in a “stable” good period.

3. FORECASTING

As shown in previous studies because of the wide fluctuations that Ka-band signal could incur due to weather effects [3][4][6][7], weather forecasting - or more accurately link forecasting- could be used to improve both data return and link continuity. Currently, DSN is exploring the use of forecasts generated by the Spaceflight Meteorology Group at Johnson Space Flight Center [13]. These forecasts, originally intended for use by NASA’s Space Shuttle program, give a detailed multi-layer meteorological description of the atmosphere including details such as pressure, temperature, dew

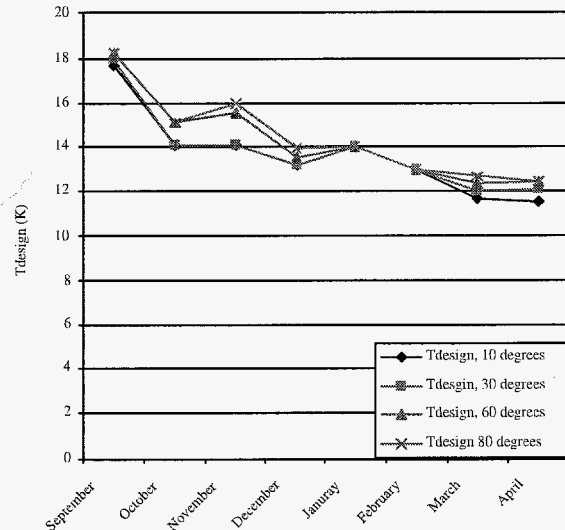


Figure 1. Monthly Link Design T_z for Goldstone

point, absolute humidity and liquid water content every six hours from 12 to 120 hours into the future. Therefore, each forecast *set* includes 19 different forecast *types*. (A forecast 30 hours into the future is of a different *type* than a forecast 36 hours into the future). Each forecast is valid for a single point in time; however, for our purposes, they could be taken as representative of the six-hour period centered around them. For the period of the study reported on in this paper, only forecasts for Goldstone were available.

Each forecast is used to generate an estimate of the zenith atmospheric noise temperature based on standard weather models (*e.g.* [14]). As expected the forecast accuracy decreases as weather is forecast further into the future. Furthermore, because of ambiguity in the way the cloud effects are represented in these forecasts, presence of clouds cause the estimation of the atmospheric noise temperature to be unnecessarily large. However, in general, if an atmospheric noise temperature value calculated from one forecast is larger than another value from another forecast (of the same type), then the actual atmospheric noise temperature during the time of the first forecast is larger than the atmospheric noise temperature during the time of the forecast with lower predicted atmospheric noise temperature. Therefore, the atmospheric noise temperature values calculated from these forecasts could be used as *channel quality* forecasts.

Since the forecasts are valid only for a single point in time and there are uncertainties regarding estimation of cloud effects, a “calibration” process has been used to make the forecasts useful. The first step in this process is to specify a “calibration” period starting at time t_s and ending t_f . Over

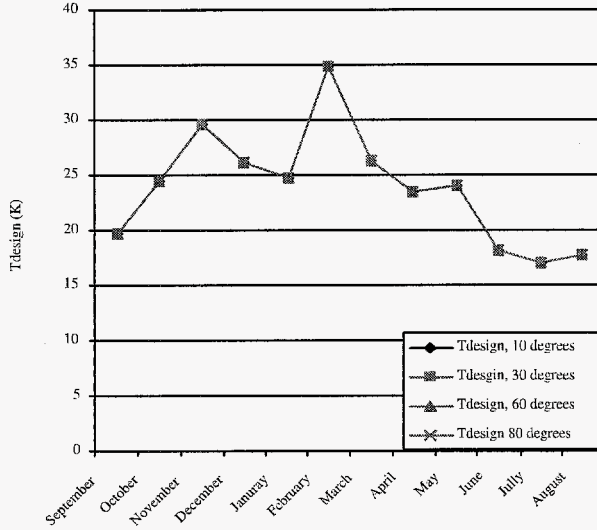


Figure 2. Monthly Link Design Zenith Atmospheric Noise Temperatures for Canberra

this period there are N_K channel quality values for forecasts of type K . Since the channel quality values are based on a random process (namely the weather) then the channel quality value for a forecast of type K is a random variable (call it $Q^{(K)}$). From the instances of this random variable, $\left(\left\{q_i^{(K)}, 1 \leq i \leq N_K\right\}\right)$, over the calibration period we can calculate a distribution for channel quality values of type K , $F_K(q) = \Pr\{Q^{(K)} < q\}$.

Let $t_i^{(K)}$ be the time of the i th forecast of type K . The associated time period with this forecast is the time interval $\left(t_i^{(K)} - 3, t_i^{(K)} + 3\right)$. Given this and $F_K(q)$ we can categorize observations of T_z obtained by the Advanced Water Vapor Radiometer (AWVR). Let $T_z(t)$ be the zenith atmospheric noise temperature value that the AWVR is measuring at time t . Then for forecasts of type K we can define the sets of AWVR data for type K forecasts, $S_n^{(K)}$ in the following manner:

$$S_n^{(K)} = \left\{T_z(t) \mid t \in \left(t_i^{(K)} - 3, t_i^{(K)} + 3\right) \text{ and } 0.05(n-1) \leq F_K(q_i) < 0.05n\right\} \quad (3)$$

Let $F_K^{(n)}(T_z)$ be the distribution that is obtained for zenith atmospheric noise temperature measurements in $S_n^{(K)}$. These distributions along with $F_K(q)$ are used to generate conditional atmospheric noise temperature distributions for future forecasts. Let q be the channel quality value that a forecast of type K after the calibration period generates. Then the link could be designed according the atmospheric noise tempera-

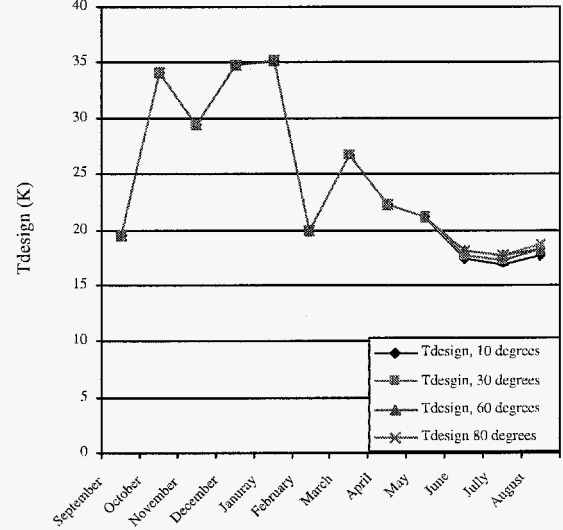


Figure 3. Monthly Link Design Zenith Atmospheric Noise Temperatures for Madrid

ture distribution, $F_K(T_z, q)$ where

$$F_K(T_z, q) = F_K^{(n)}(T_z) \ni 0.05(n-1) \leq F_K(q) < 0.05n \quad (4)$$

Note that this process is identical to the process through which monthly T_z statistics are calculated, except that with monthly statistics, instead of a channel quality value, the month over which the T_z measurements have taken place is used to categorize the AWVR data. Finally, it should be noted that based on our analysis of the forecasts, the “fresher” the forecast (*i.e.*, it projects a shorter time into the future) the more accurate it is. Therefore, for the analysis presented in this paper, always the “freshest” forecast is used.

4. RESULTS AND DISCUSSION

The continuity and completeness analysis was performed for the three DSN communication complex: Goldstone, California; Canberra, Australia and Madrid, Spain. The data from the AWVR at Goldstone and Water Vapor Radiometer (WVR) for Canberra and Madrid were used for the T_z time series for this analysis. For Goldstone this analysis was performed with both forecasting and long term monthly statistics. Although analysis based on long term statistics could have been performed until August 2004, the forecasts were not processed beyond April 2004; therefore, in order to have a fair comparison between a link designed with forecasting and a link designed using long-term statistics the analysis was limited to the period from September 2003 to April 2004. For Canberra, the analysis using monthly statistics was performed from September 2003 through August 2004 except for March and April 2004. During those months the WVR at

Canberra was not available due to repairs. For Madrid, the WVR data from September 2003 through August 2004 was used for the analysis. It should be noted that this analysis was “blind,” *i.e.* none of the WVR or forecasts used for the analysis was used to obtain atmospheric noise temperature distributions that were used for the link design. Therefore, the analysis presented here is a true measure of the continuity/completeness of the link.

Continuity and Completeness of the Ka-band Link Designed according to Long-term Statistics

The first step in our analysis of the link designed with long-term statistics was the calculation $T_z^{(0)}(\theta)$ at different elevations for different months at each of the DSN complexes. For these calculations, $T_z^{(0)}(\theta)$ is selected such that the average data return over a 34-m Beam Waveguide (BWG) [8] is maximized at the given elevation subject to a minimum of 90% availability. The results of this exercise are shown in Figs. 1 through 3. As seen from these figures, none of the site displays any significant variation in $T_z^{(0)}(\theta)$ as a function of elevation. Therefore, in terms of continuity and completeness the only Goldstone would display any variation as a function of elevation. Therefore, all the figures that will be discussed in this paper will focus on 30 deg. elevation results as they are representative of the continuity of the link at all elevations.

Using these $T_z^{(0)}(\theta)$ values continuity and completeness statistics and the link stability for the three sites were calculated. These results are presented in Tables 1 through 3 and in Figs. 4 through 6. As seen from Tables 1 through 3 and Figs. 4 and 5, while the availability of the link for all three sites for the same elevation are roughly the same, the distribution of good periods and bad periods are different for each complex. Goldstone has large averages for good period durations and also large standard deviations for them. Canberra has slightly smaller averages for good period durations compared to Goldstone. It also significantly smaller standard deviations for them. Madrid has much smaller averages for good period durations than either Goldstone or Canberra but it has standard deviations similar to Canberra. As far as bad periods are concerned, Goldstone has larger averages for bad period durations as well as larger standard deviations for them. Madrid has the smallest average durations of bad periods while Canberra has averages for bad period durations somewhere between Madrid and Goldstone. Both Madrid and Canberra has much smaller standard deviations for bad period durations than Goldstone. Looking at the distributions of good periods and bad periods, the reason for this becomes obvious. The distributions for Goldstone indicate that both for good periods and bad periods there are some very short duration events and some very long duration events. This causes both the mean and the standard deviations to be large. For Madrid, the distributions are dominated by short duration events, therefore, both the means and the standard deviations are small. Canberra’s distribution (compared to Goldstone’s and Madrid’s) seemsto have more longer du-

Table 1. Completeness and Continuity Statistics for Goldstone

El. (deg)	Avail.	Avg. Good period (hrs)	Sd. Good period (hrs)	Avg. Bad period (hrs)	Sd. Bad period (hrs)
10	0.895	9.688	39.33	1.252	4.870
30	0.900	9.376	38.69	1.136	3.583
60	0.917	9.387	38.63	0.9957	3.214
80	0.914	9.432	38.68	0.9680	2.990

Table 2. Completeness and Continuity Statistics for Canberra

El. (deg)	Avail.	Avg. Good period (hrs)	Sd. Good period (hrs)	Avg. Bad period (hrs)	Sd. Bad period (hrs)
10	0.911	7.698	17.47	0.8396	1.903
30	0.911	7.698	17.47	0.8396	1.903
60	0.911	7.698	17.47	0.8396	1.903
80	0.911	7.698	17.47	0.8396	1.903

ration events (but not too long) and that causes the standard deviations to be smaller than Goldstone’s and the means to be larger than Madrid’s.

The means and the standard deviations also indicate that the link over at Goldstone is relatively more “stable” than the links over at Canberra and Madrid and that Canberra’s link is more “stable” than Madrid’s. This is because Goldstone has more longer duration events in its distributions than either Madrid or Canberra and Madrid has more shorter duration events in its distributions than either Canberra or Goldstone. This conclusion is also supported by Fig. 6. As seen from this figure, Goldstone has better stability than the other two sites and Canberra has slightly better stability than Madrid. Also note that based on this figure, for all three sites at least 80% of the time the link is in a “good” period that is at least 8 hours long (typical duration of a DSN pass). This indicates

Table 3. Completeness and Continuity Statistics for Madrid

El. (deg)	Avail.	Avg. Good period (hrs)	Sd. Good period (hrs)	Avg. Bad period (hrs)	Sd. Bad period (hrs)
10	0.894	2.233	17.04	0.2678	1.407
30	0.901	2.435	17.83	0.2681	1.402
60	0.905	2.602	18.43	0.2754	1.433
80	0.907	2.615	18.49	0.2712	1.419

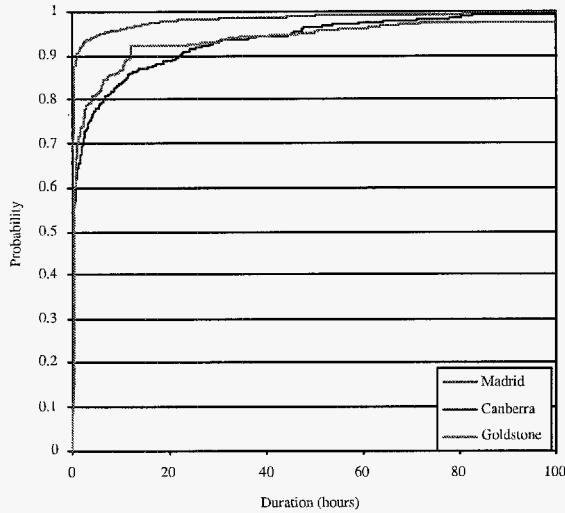


Figure 4. “Good” Period Cumulative Distribution; 30 deg. Elevation; Long-term Statistics Link Design.

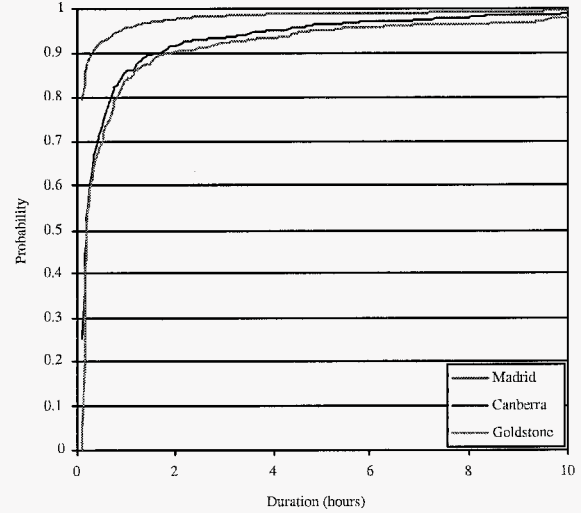


Figure 5. “Bad” Period Cumulative Distribution; 30 deg. Elevation; Long-term Statistics Link Design.

that while the stability of the Ka-band link varies from site to site, in general, the Ka-band link designed with long-term statistics is rather stable.

Continuity and Completeness of the Ka-band Link with Forecasting

The results of the analysis of the continuity and completeness for the Ka-band link with forecasting is presented in Tables 4 through 6 and in Figs. 7 through 10. Again it should be noted that $T_z^{(0)}(\theta)$ values were selected so that the link would have the maximum average data return at the given elevation over a 34-m BWG antenna with a minimum of 90% availability given the forecast. When Table 4 is compared to Table 1 it is observed that while the averages for good period durations slightly decrease with forecasting, the averages for bad period duration and the standard deviations of both the good and bad period durations significantly decrease. In addition, the availability of the link slightly improves with forecasting. Table 5 indicates that all this occurs with a slight improvement in the link’s data return (approximately 5%). This is because of the fact that with forecasting the link is designed according to the actual dynamics of the link, thus preventing very long bad periods or very long good periods from occurring (see Fig. 10). This in turn reduces the standard deviation of both the good periods and the bad periods. This observation is further supported by the results in Table 6. As seen from this table, the 99-percentile values for both the good periods and the bad periods are significantly reduced through forecasting. In addition, forecasting seems to reduce the number of relatively short good periods as shown in Fig. 7.

Finally, forecasting improves the short-term stability of the

Table 4. Completeness and Continuity Statistics for Forecasting at Goldstone

El. (deg)	Avail.	Avg. Good period (hrs)	Sd. Good period (hrs)	Avg. Bad period (hrs)	Sd. Bad period (hrs)
10	0.916	8.291	25.01	0.8334	1.729
30	0.926	8.460	25.68	0.7402	1.446
60	0.932	9.271	27.00	0.7494	1.430
80	0.933	9.387	27.18	0.7514	1.437

link. As seen from Fig. 9 the stability of the link under 10 hours is better with forecasting. As a typical DSN pass 8 hours or less, this means that forecasting could significantly reduce the uncertainty in the link by improving the link’s stability and improve its continuity.

5. CAVEATS

While the work presented here indicates that our proposed Ka-band link design approach has good continuity and completeness characteristics and that these characteristics could be improved through forecasting, several issues have not been addressed.

First of all, the concept of accepting some data loss in order to maximize the average data return is something that most deep missions are not used to. Practically all deep space missions so far have based their primary science phase on the concept of having certain amount of data down from the spacecraft at a certain time. This practically requires the link to be 100%

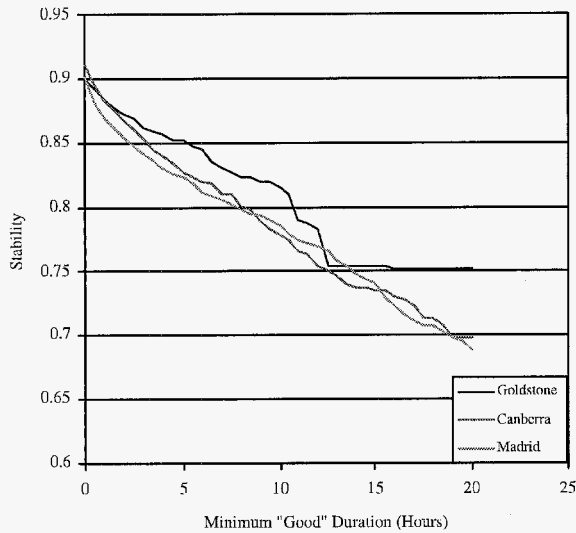


Figure 6. Link Stability vs. the Minimum Duration of the “Good” Period; 30 deg. Elevation; Long-term Statistics Link Design

Table 5. Forecasting Data Return Advantage; Goldstone

Elevation	Forecasting Advantage (dB)
10	0.425
30	0.272
60	0.233
80	0.224

available. Therefore, forcing the acceptance of 10% down time on the link on deep space missions is quite difficult. In addition, the fact that the approach presented in this paper does not provide a guaranteed latency in data return will not sit well with most missions.

Furthermore, the analysis presented here with forecasting assumed that the latest available forecasts are always used to design the link. This means that the link needs to be configured as late as 9 hours before the actual pass. Putting aside the fact that an uplink may not be available to configure the link at the desired time, most missions have long command built and review cycles of at least a week or so. This means that while the forecasts are useful, due the length of command built and review process, channel forecasting may be impossible to implement.

Finally, the performance of forecasting was analyzed only for Goldstone which has the best weather of all three DSN complexes. Madrid and Canberra both have worse weather than Goldstone, and forecasting could be better evaluated if its performance could be measured for these two complexes.

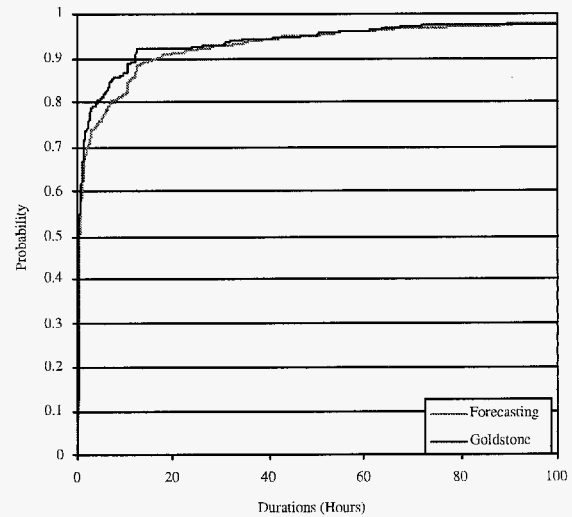


Figure 7. “Good” Period Cumulative Distribution for Goldstone; 30 deg. Elevation; Long-term Statistics and Forecasting.

Table 6. Comparison of 99-percentile Distribution Values for Forecasting and Long-term Statistics; 30 deg. Elevation, Goldstone

Link Design Approach	99-percentile Good Period (hours)	99-percentile Bad Period (hours)
Long-term	189	20
Forecasting	139	7.75

6. CONCLUSIONS

In this paper we have presented a method for analyzing the continuity and completeness of a deep space communications link using the concept of “stability.” Using this concept we have analyzed the continuity and completeness performance of a Ka-band link design based on the concept of maximizing the average data return over the link while maintaining a minimum availability. This approach was used both with long-term statistics and with forecasting. The analysis has shown that a Ka-band link designed according to this concept is relatively stable and has good completeness and continuity characteristics for all three DSN communication complexes. In addition, it was shown that forecasting improves the completeness and data return on the link slightly while significantly improving the continuity of the link.

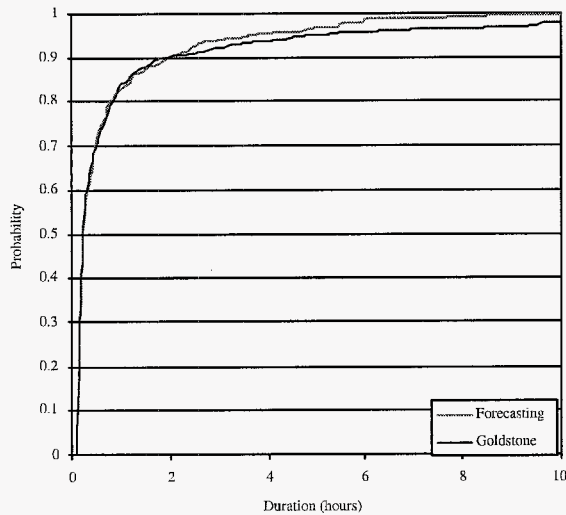


Figure 8. “Bad” Period Cumulative Distribution for Goldstone; 30 deg. Elevation; Long-term Statistics and Forecasting.

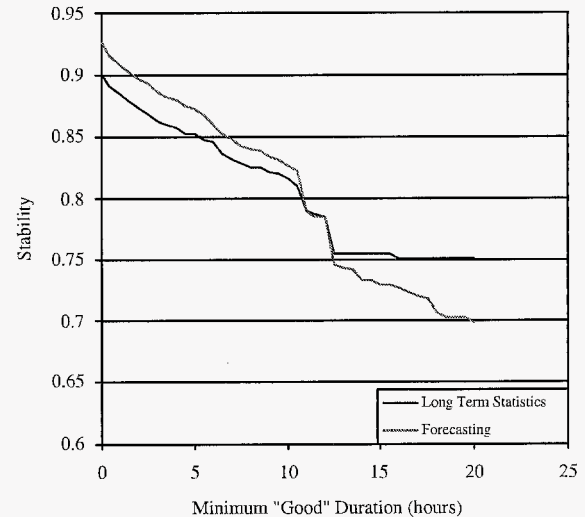


Figure 9. Link Stability vs. the Minimum Duration of the “Good” Period for Goldstone; 30 deg. Elevation; Long-term Statistics and Forecasting.

ACKNOWLEDGMENTS

This work was performed at Jet Propulsion Laboratory, California Institute of Technology, under a contract with National Aeronautics and Space Administration. The authors would like to thank David Morabito, Julian C. Breidenthal and Wallace Tai of Jet Propulsion Laboratory for providing programmatic support for the work presented here.

REFERENCES

- [1] Shambayati, S., “Optimization of a Deep-Space Ka-Band Link Using Atmospheric-Noise-Temperature Statistics,” *TMO Progress Report 42-139*, July-September 1999, pp. 1-16, Jet Propulsion Laboratory, Pasadena, CA, November 15, 1999.
- [2] Shambayati, S., “Maximization of Data Return at X-Band and Ka-Band on the DSN’s 34-Meter Beam-Waveguide Antennas,” *IPN Progress Report 42-148*, October-December 2001, pp. 1-20, February 15, 2002.
- [3] Shambayati, S., “On the Use of W-Band for Deep-Space Communications,” *IPN Progress Report 42-154*, April-June 2003, pp. 1-17, Jet Propulsion Laboratory, Pasadena, CA, August 15, 2003.
- [4] Shambayati, S., “On the Benefits of Short-term Weather Forecasting for Ka-band (32 GHz),” *IEEE Aerospace Conference*, Big Sky, Montana, March 7-12, 2004
- [5] Shambayati, S., Davarian, F., Morabito, D., “Link Design and Planning for Mars Reconnaissance Orbiter (MRO) Ka-band (32 GHz) Telecom Demonstration,” *IEEE Aerospace Conference*, Big Sky, Montana, March 5-12, 2005.
- [6] Davarian, F., Shambayati, S., Slobin, S., “Deep Space Ka-Band Link Management and the MRO Demonstration: Past Statistics versus Forecasting,” *Proceedings of IEEE*, December 2004.
- [7] Davarian, F., Shambayati, S., Slobin, S., “Ka-band Link Management for Deep Space Applications,” *10th Ka and Broadband Communications Conference*, Venice, Italy, Sept. 30- Oct. 2, 2004.
- [8] Sniffin, R. W., Ed., *DSMS Telecommunications Link Design Handbook (810-005, Rev. E)*, Module 301, Rev. B: Coverage and Geometry, <http://deepspace.jpl.nasa.gov/dsndocs/810-005/301/301B.pdf>, Jet Propulsion Laboratory, Pasadena, CA, February 4, 2004.
- [9] Morabito, D. D., Shambayati, S., Butman, S., Fort, D., and Finley, S., “The 1998 Mars Global Surveyor Solar Corona Experiment,” *The Telecommunications and Mission Operations Progress Report 42 142*, April-May 2000, Jet Propulsion Laboratory, Pasadena, California, August 15, 2000.
- [10] Morabito, D. D., Shambayati, S., Finley, S., Fort, D., Taylor, J. and Moyd, K., “Ka-band and X-band Observations of the Solar Corona Acquired During Solar Conjunctions of Interplanetary Spacecraft,” *Proceedings of the 7th Ka-band Utilization Conference*, September 26, 2001, Santa Margherita Ligure, Italy. IIC - Istituto Internazionale delle Comunicazioni, Via Perinace - Villa Piaggio, 16125 Genova, Italy.

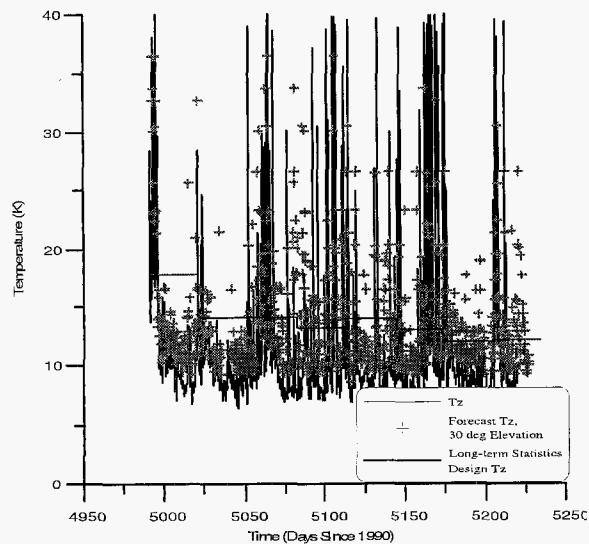


Figure 10. Goldstone AWVR measured T_z , Forecast T_z and Long-term Statistics Design T_z

I Ka-band testing and 70m antenna Ka-band Task. Currently, Dr. Shambayati is the Principal Investigator for the Mars Reconnaissance Orbiter Ka-band Demonstration. His current research interests and activities include evaluating the effects of weather outages on the spacecraft resources, Ka-band weather forecasting, Ka-band link design and engineering support for implementation of Ka-band services in NASA's Deep Space Network.

- [11] Morabito, D., Shambayati, S., Finley, S. and Fort, D., "The Cassini May 2000 Solar Conjunction," *IEEE Transactions on Antennas and Propagation*, Vol. 51, No. 2, February 2003, pp. 201-219.
- [12] Morabito, D. D., and Hastrup, R., "Communicating with Mars During Periods of Solar Conjunction," *Proceedings of the 2002 IEEE Aerospace Conference*, Big Sky, Montana, March 9-16, 2002.
- [13] NOAA National Weather Service Spaceflight Meteorology Group, <http://www.srh.noaa.gov/smg>.
- [14] Ulaby, F. T., Moore, R. K. and Fung, A. K., *Microwave Remote Sensing: Active and Passive, Volume I: Fundamentals and Radiometry*, Artech House Publishers, March 1986.



Shervin Shambayati obtained his Bachelors of Science degree in Applied Mathematics and Engineering in 1989 from California State University, Northridge. Subsequently, he obtained his MSEE, Engineer's Degree and Ph.D. from University of California, Los Angeles in 1991, 1993 and 2002, respectively.

In 1993, Dr. Shambayati joined the Deep Space Communications Systems Group at Jet Propulsion Laboratory where he took part in development and testing of Deep Space Network's Galileo Telemetry receiver (DGT). In 1997, Dr. Shambayati joined the Information Processing Group at JPL where he has been working ever since. With that group Dr. Shambayati has been involved in various projects including Mars Global Surveyor's Ka-Band Link Experiment II, Deep Space